Telocytes in the human kidney cortex

Guisheng Qi [a, b, #], **Miao Lin** [a, b, #], **Ming Xu** [a, b], **C. G. Manole** [c], **Xiangdong Wang** [d], **Tongyu Zhu** [a, b, *]

[a] *Department of Urology,*
[b] *Shanghai Key Lab of Organ Transplantation,*
[c] *Department of Cellular ad Molecular Medicine, University of Medicine, Bucharest &*
National Institute of Pathology, Bucharest, Romania
[d] *Biomedical Research Center, Fudan University Zhongshan Hospital, Shanghai, China*

Abstract

Renal interstitial cells play an important role in the physiology and pathology of the kidneys. As a novel type of interstitial cell, telocytes (TCs) have been described in various tissues and organs, including the heart, lung, skeletal muscle, urinary tract, *etc.* (www.telocytes.com). However, it is not known if TCs are present in the kidney interstitium. We demonstrated the presence of TCs in human kidney cortex interstitium using primary cell culture, transmission electron microscopy (TEM) and *in situ* immunohistochemistry (IHC). Renal TCs were positive for CD34, CD117 and vimentin. They were localized in the kidney cortex interstitial compartment, partially covering the tubules and vascular walls. Morphologically, renal TCs resemble TCs described in other organs, with very long telopodes (Tps) composed of thin segments (podomers) and dilated segments (podoms). However, their possible roles (beyond intercellular signalling) as well as their specific phenotype in the kidney remain to be established.

Keywords: telocytes ● telopodes ● human kidney cortex ● interstitial cells ● CD34 ● CD117

Introduction

Telocytes (TCs) are a distinct interstitial cell population, first described in 2010 [1, 2]. They are found in several mammalian and human organs [3–20]. The main characteristic of TCs is the presence of telopodes (Tps), visible using electron microscopy. Tps are composed of alternating thin segments (podomers) and thick segments (podoms). Renal interstitial cells are involved in many diseases, such as acute interstitial nephritis [21], chronic allograft rejection [22] and ischaemia reperfusion injury [23]. Traditionally, fibroblasts and immune cells are considered the main interstitial cells in kidneys [24, 25]. However, renal stromal cells have great morphological plasticity. In the past, these cells were arbitrarily called 'fibroblasts', despite the fact that the main function of fibroblasts is structural (to produce collagen and collagen fibrils). In normal kidney cortex interstitium, collagen is not at all abundant. This could suggest that the kidney interstitial cells are heterogeneous in their phenotype. Up to date,

there are no reports regarding the presence of TCs in the kidney interstitium. This study aimed to investigate the presence of TCs in the human kidney cortex, using primary cell culture, vital cell staining with Janus Green B, mitochondrial labelling using Mito Tracker Green, immunocytochemistry, transmission electron microscopy (TEM), and *in situ* immunohistochemistry (IHC).

Materials and methods

Tissue samples

Human kidney cortex samples were obtained from five patients, aged 40–64 years, who suffered from malignant kidney tumours and consented to radical nephrectomy. The non-neoplastic parts of the resection specimens were confirmed by morphopathology and used for this study.

Cell culture

Sterile samples were minced into small pieces of about 1 mm³ and washed three times with phosphate-buffered saline (PBS, Gibco, Portland, Oregon, USA). Samples were further digested for 4 hrs on an orbital

---
[#]These authors have equal contribution to this work.
*Correspondence to: Tongyu ZHU, MD, PhD, Prof,
Department of Urology,
Fudan University Zhongshan Hospital,
Shanghai, China.
Tel.: +86 21 64041990 (ext. 5468)
Fax: +86 21 64037269
E-mail: tyzhu@fudan.edu.cn

shaker at 37°C, with 10 mg/ml collagenase type II (Sigma-Aldrich, St. Louis, Missouri, USA) and 2000 U/ml deoxyribonuclease I (Sigma-Aldrich) in PBS, without Ca^{2+} and Mg^{2+}. Dispersed cells were collected by centrifugation at 284 × **g** and separated by filtration through 40 μm diameter cell strainers (BD Falcon, San Jose, CA, USA). Cells were cultured in DMEM/F12 (Gibco, Portland, Oregon, USA), supplemented with 10% FBS. The medium was changed every 48 hrs and a phase contrast microscope (Olympus 1x51; Olympus, Tokyo, Japan) was used to observe the growth of TCs.

Staining and mitochondrial labelling of cultured cells

Cells were washed in pre-warmed phenol red-free DMEM, and incubated in 0.02% Janus Green B (Sigma-Aldrich) for 30 min. Mito Tracker Green FM (Beyotime, Haimen, China), a lipophilic, selective dye that can be concentrated by active mitochondria, was used for mitochondrial labelling. Cells were incubated in 100 nmol/l Mito Tracker Green for 30 min. TCs were examined and photographed using fluorescence microscopy (450–490 nm excitation light, 520 nm barrier filter, Olympus 1x51; Olympus).

Immunocytochemistry

Cells grown on cover slips were fixed in 4% paraformaldehyde for 10 min., cold preserved over night at 4°C, then incubated in PBS for another 30 min. at room temperature. Cells were then incubated in 5% BSA in PBS for 1 hr at room temperature. The cells were incubated with the primary antibodies for 60 min. at 37°C, using rat anti-human CD34 (1:100; Santa Cruz, Santa Cruz, CA, USA), rabbit anti-human CD117 (1:10; Abcam, Cambridge, UK), and rabbit anti-human vimentin (1:200; Abcam). After three serial rinses with PBS, the primary antibodies were detected with secondary antibodies conjugated to fluorescein isothiocyanate (FITC) or tetraethyl rhodamine isothiocyanate (TRITC; Jackson, Lancaster, PA, USA). Finally, the nuclei were counterstained with 1 mg/ml 4′, 6-diamidino-2-phenylindole (DAPI) (Sigma-Aldrich). Negative controls were obtained by following the same protocol while omitting the primary antibodies. Samples were examined under a phase contrast microscope (Olympus BX51; Olympus) equipped with appropriate fluorescence filters.

Transmission electron microscopy

Human kidney samples were obtained using a lateral, cutting through-type autobiopsy gun (MG15-22; Bard, Murray Hill, NJ, USA) before the renal vascular pedicle was clamped during radical nephrectomy. Tissue samples were initially fixed in 2.5% glutaraldehyde in 0.1 M phosphate buffer (pH 7.2), then post-fixed in 1.0% OsO_4 (Polysciences Inc., Niles, Illinois, USA) for 1 hr. Samples were then rinsed extensively in dd$H_2$0, dehydrated in a graded series of ethanol, and embedded in Eponate 812 resin (Ted Pella Inc., Redding, CA, USA). The embedded samples were dried by heat with a graded temperature. Then, sections of 50 nm were cut using a Leica Ultracut UCT ultramicrotome (Leica Microsystems Inc, LKB-II, Germany), stained with a 3% solution of uranyl acetate and lead citrate, and mounted on formvar-coated 50 mesh grids. Prepared tissue

samples were observed using a TEM (Philips model CM120; Philips, Amsterdam, Holland). Digital pictures (2048 × 2048 pixels, 4 MB, and uncompressed grayscale TIFF files) were obtained using a high resolution ratio digital camera connected to the TEM.

In situ immunohistochemistry

Samples were fixed in 4% formalin and embedded in paraffin according to routine histology protocols. Sequential 5 μm sections were deparaffinized in xylene, hydrated in alcohol series, and washed in phosphate-buffered solution at pH 7.4. Antigen retrieval was performed by heating in TRIS-citrate buffer for 40 min. at 96°C. The sections were set aside to reach room temperature, and then washed in PBS. Endogenous peroxidase blocking was completed using 3% H_2O_2-methanol, and then the sections were incubated in 5% BSA for 30 min. The primary antibodies used were the following: CD117 (1:50; Abcam), vimentin (1:500; Abcam), CD34 (1:200; Santa Cruz), CD31 (1:100; Dako, Glostrup, Denmark), D2–40 (1:200; Dako, Glostrup, Denmark), and tryptase (1:100; Abcam). CD31 and D2–40 were used to exclude endothelial staining of CD34 [26, 27] and tryptase to exclude mast cell staining of CD117 [28].

Sections were incubated with primary antibody at 4°C overnight and HRP-conjugated secondary antibodies for 60 min. at room temperature. Then, they were stained with 3, 3′–diaminobenzidine followed by haematoxylin counterstaining. The same areas of serial sections were observed and photographed using an Olympus microscope (1 × 71) equipped with a digital camera (Olympus dp72; Olympus). Negative controls were obtained by following the same protocol while omitting the primary antibodies. Positive controls were obtained using gastrointestinal stromal tumour samples expressing CD117, CD34 and vimentin.

Results

Cell culture

Under phase contrast microscope, we observed spindle-shaped cells with long, thin, and moniliform prolongations. As shown in Figure 1A, a characteristic cell has one long, thin, and moniliform prolongation consisting of alternating thin and thick segments (podomers and podoms respectively). Another cell with several such prolongations was also observed (Fig. 1B). The shapes of cell bodies changed from pyriform (Fig. 1A) to polygonous (Fig. 1B) depending on the number of prolongations. These cells closely resemble the TCs described in other organs, suggesting the presence of TCs in the human kidney cortex.

Vital cell staining and mitochondrial labelling

Both Janus Green B (Fig. 2A) and Mito Tracker Green (Fig. 2B) illustrated the high concentration of mitochondria in the cultured cells. When compared to the thin segments (podomers), the dilated segments (podoms) of the prolongations have brighter fluorescent signals (Fig. 2B). Our evaluation of the human kidney cortex demonstrated a greater concentration of mitochondria within the thick
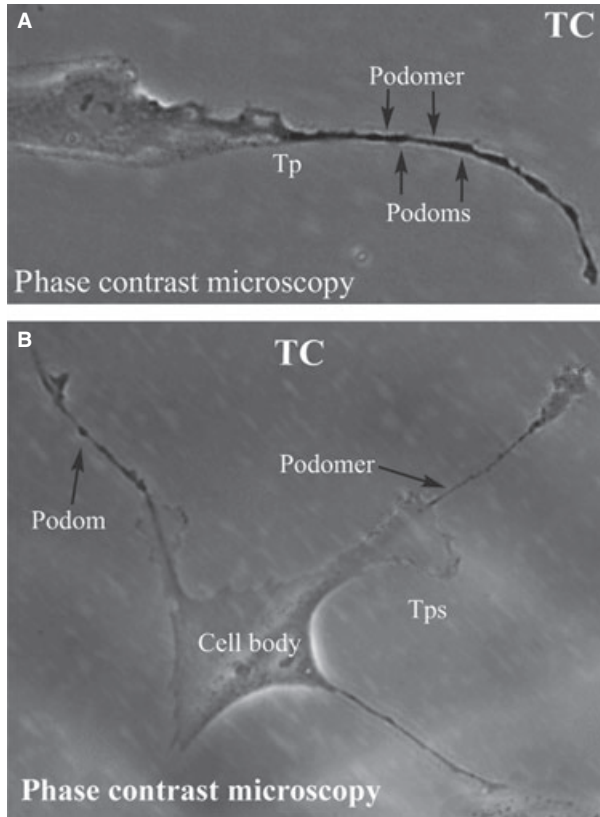
Fig. 1 (**A**) and (**B**) Phase contrast microscopy of kidney TCs in primary culture. Note the typically very long Tps (over 50 μm). Also, the specific structure of Tps is obvious: alternation of dilations (podoms) with thin segments (podomers). Direct magnification: 400×. TC: Telocyte; Tp: Telopode.

Fig. 2 (**A**) and (**B**) Kidney TCs in primary culture. (A) Vital staining for mitochondria with Janus Green B; note the podoms coloured blue-brown because of the presence of mitochondria. (B) Fluorescence microscopy using Mito Tracker Green as molecular probe for the presence of mitochondria; note the moniliform aspect of Tps as a result of accumulation of mitochondria in podoms. TC: Telocyte; Tp: Telopode; Mito Tracker G: Mito Tracker Green.

segments of prolongations and around the nucleus (Fig. 2), as previously demonstrated by Popesu *et al.* in TCs from different organs [6, 8, 9]. This similarity of mitochondrial distribution may suggest possible roles for kidney TCs.

Immunocytochemistry

The cultured cells positively expressed CD117, CD34 and vimentin (Fig. 3). The alternating thick and thin segments of their prolongations are shown by fluorescence (Fig. 3A and C). Staining with CD34 (Fig. 3B) did not have the same colour as staining with CD117 (Fig. 3A), when both were labelled with FITC, as the fluorescence colour appeared yellowish compared with CD117 staining. This phenomenon might be related to expression differences between CD34 and CD117.

Transmission electron microscopy

Cells with long, thin, and moniliform prolongations in the human kidney cortex interstitium are shown in Figures 4A and 5A. These cells
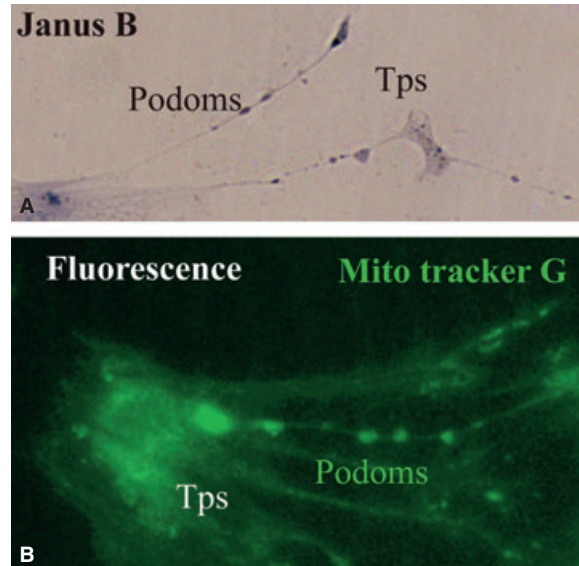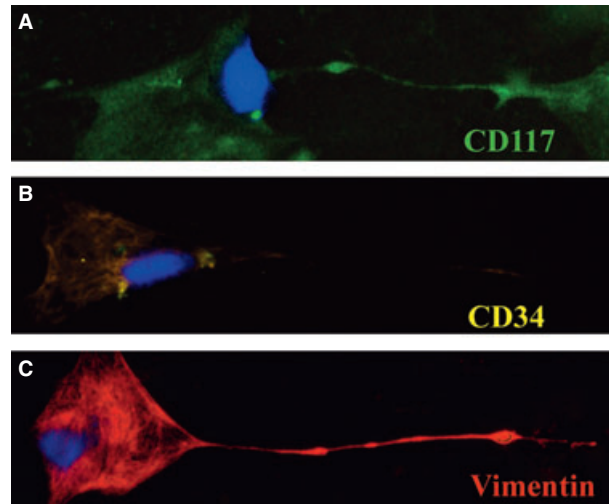

Fig. 3 Immunofluorescence labelling for CD117, CD34 and vimentin of cultured cells. (**A**) FITC labelling for CD117 (green). (**B**) FITC labelling for CD34 (yellow). (**C**) TRITC labelling for vimentin (red). DAPI staining for nuclei (blue) in (A), (B), and (C). FITC: fluorescein isothiocyanate; TRITC: tetraethyl rhodamine isothiocyanate; DAPI: 4′, 6-diamidino-2-phenylindole.

Fig. 4 TEM image of kidney telocyte. There is a typical telocyte between a tubule and a vessel (**A**). Mitochondrion and lamellar body are found near nuclear (**B**). Shed vesicle and caveola could also be found after magnification (**C**) and (**D**). TC: telocyte; Tp: telopode; RBC: red blood cell; E: endothelium; BM: basement membrane.
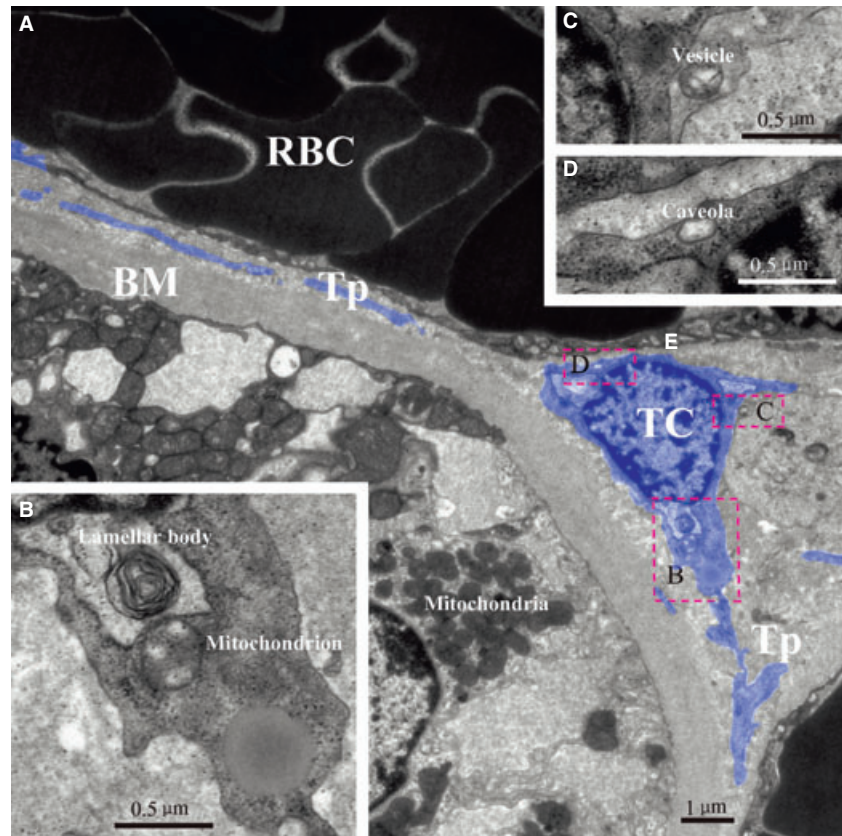
are located around tubules and vessels with their prolongations wrapping around the endothelium (Figs 4 and 5). The prolongations suddenly emerge from cell bodies and are extremely long and very sinuous. The dilated segment of the prolongation is clearly displayed in Figure 5C. The mitochondria, lamellar body, microfilaments, caveolae and vesicle are seen in high magnification images (Figs 4B–D and 5B, C). Other organelles, such as the rough endoplasmic reticulum, Golgi body and ribosomes, are rarely seen in our images. These cells tend to have more than one prolongation *in vivo*. Their shapes change

from spindle to triangular, depending on the number of prolongations.

In situ immunohistochemistry

Immunostaining of CD117, CD34, vimentin, CD31, D2–40 and tryptase of the same area on serial sections of cortex are shown in Figure 6. According to our results, cells with a typical TC morphology,

Fig. 5 TEM image of kidney telocyte. A typical telocyte with Tps is around a blood capillary located in kidney interstitium (**A**). Note Tps which prolong along the basement membrane of vessel. Details of its podomer and podom are presented (**B**) and (**C**). Shed vesicle is next to podomer and obvious mitochondria are next to nuclear (B). In podom, there are microfilaments and vesicle (C). TC: telocyte; RBC: red blood cell; E: endothelium; BM: basement membrane.
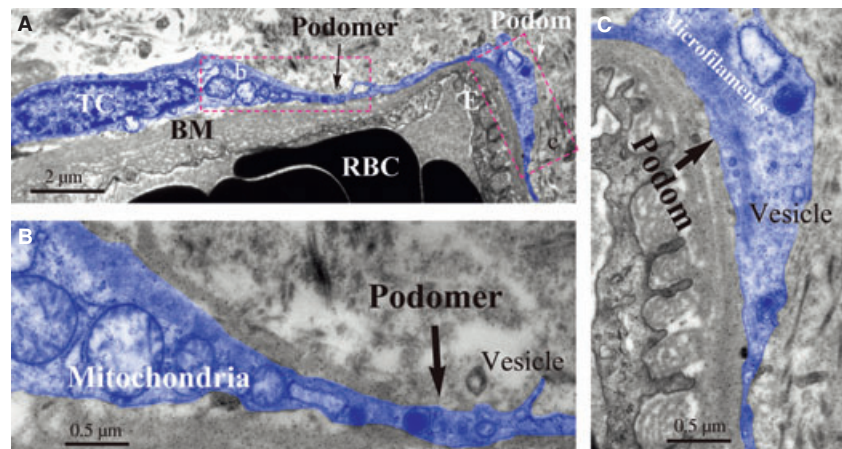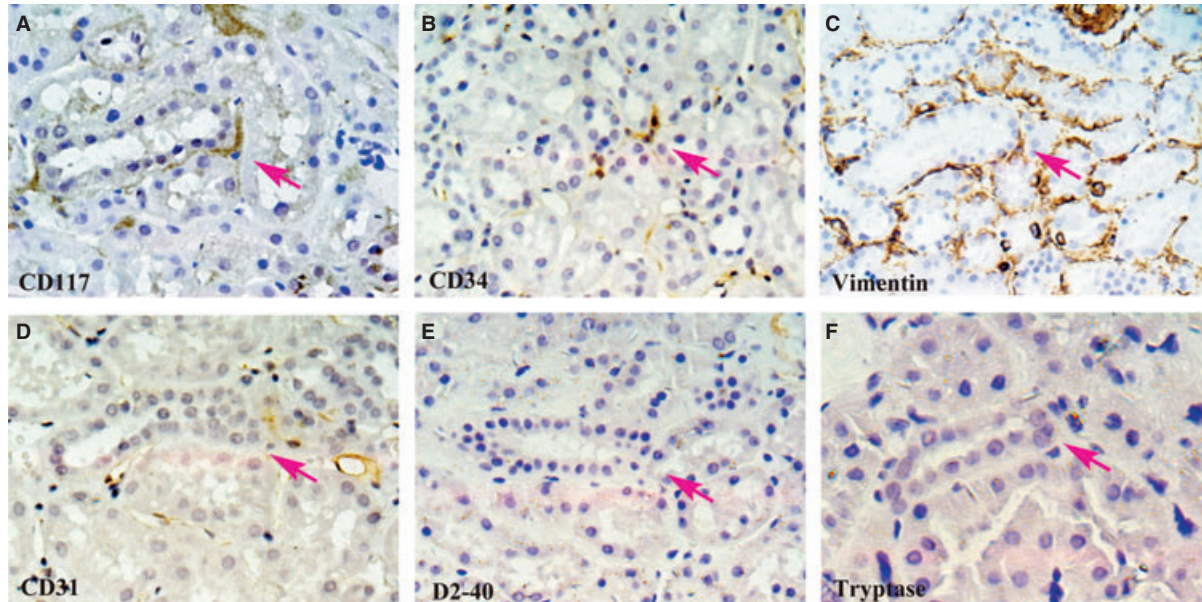
Fig. 6 *In situ* IHC of CD117, CD34, vimentin, CD31, D2–40 and Tryptase on serial slides. One cell with positive expression of CD117 can be seen in the kidney interstitium (**A**; magenta arrow). It has three long and thin Tps. Positive expressions of CD34 and vimentin can be observed in the same area of serial slides (**B**) and (**C**). Staining results of CD31, D2–40 and tryptase are presented (**D**)–(**F**) on serial slides. Their negative expressions in same area help us exclude mast cell staining of CD117 and endothelial cell staining of CD34. Magnification: 400×.

and with positive expression for CD117 (Fig. 6A), CD34 (Fig. 6B) and vimentin (Fig. 6C) are located in the interstitium of the kidney cortex. These cells, together with their prolongations, surround renal epithelial tubules and/or vessels. They were negative for expression of CD31 (Fig. 6D), D2–40 (Fig. 6E) and tryptase (Fig. 6F), which excluded endothelia and mast cell staining. The distribution of these cells, as observed by IHC, was also confirmed by TEM.

Discussion

The presence of TCs was previously documented in different organs, including the epicardium [3], endocardium [4], myocardium [5], term placenta [6], duodenum [7], skeletal muscle [8], trachea and lung [9], vasculature [10], pleura [11], trigeminal ganglion [12], myometrium [13], endometrium [14], skin [15], urinary tract [16], parotid glands [17], meninges and choroid plexus [18], pancreas [19] and jejunum [20]. Yet, the presence of TCs has not been reported in the mammalian kidney cortex.

Our study aimed to establish whether or not TCs are present in kidney interstitium, using cell culture, TEM and IHC. Previous studies [1–20, 29] established six distinct features of TCs as the following: (1) localization within the interstitium, (2) the shape of the cell body could be pyriform, fusiform, triangular, or quadrangular, in accordance with the number of cellular prolongations (Tps), (3) having Tps: (*i*) typical prolongations, being very long and very thin, with a moniliform silhouette (alternation of podomers–thin seg-

ments–and podoms–dilated segments); (*ii*) a dichotomic branching pattern; (*iii*) inter-connected by homo-cellular junctions (but also connected with other neighbouring cells, by heterocellular junctions); (*iv*) forming a labyrinthine system, (4) podoms harbour the so-called 'calcium uptake/releasing unit', (5) positive for CD117, CD34 and vimentin, and (6) extremely low expression of microRNA-193.

Using cell culture, TEM, and *in situ* IHC, we documented that cells with a morphology similar to that described for TCs in other organs were present in the human kidney cortex interstitium. Morphologically, the cells that we isolated and identified met all the criteria previously established for TCs and for their Tps. The specific alternation of thin segments and dilated segments was observed (Fig. 1). The vital staining with Mito Tracker Green confirmed the existence of mitochondria within the dilations (Fig. 2B). These cells had positive expression of CD117, CD34 and vimentin (Fig. 3). TEM images established that these cells were located proximal to vessels and tubules in the interstitium. In some instances, their prolongations extended along the basement membrane (Figs 4A and 5A). *In situ* IHC results suggested the same distribution in the human kidney cortex (Fig. 6A–C). Negative expression of CD31, D2–40 and tryptase further confirmed the presence of TCs by excluding endothelial and mast cells (Fig. 6D–F).

Previous studies stated that kidney interstitial cells only consisted of fibroblasts, dendritic cells, macrophages and lymphocytes [24, 25]. The cells described here were also located in the kidney interstitium; although, they had characteristic prolongations (Tps) and specific biomarkers (CD117, CD34 and vimentin), which can distinguish

them from fibroblasts and other cells in both morphology and phenotype. During our research, we also obtained samples from the medulla of human kidneys and examined them through cell culture, immunocytochemistry, *in situ* IHC and TEM following the same protocols as those for the cortex. Results were contradictory. During cell culture, we found cells with the suggestive appearance of TCs. However, no typical TCs were observed in our TEM images and *in situ* IHC showed no positive expression of CD117 in the medulla. We speculate that the quantity of TCs in the medulla was insufficient for TEM and *in situ* IHC to be detected.

In conclusion, our study established the presence of TCs in the human kidney cortex interstitium, mainly locating around renal tubules and vessels. Yet, the precise function of TCs remains to be established. In several studies on TCs, potential roles have been proposed [30–32]. The specific distribution of TCs might be related to their function. Previous studies demonstrated close relationships between TCs and other cells [33–39]. In both heart [40] and skeletal muscle [41], TCs were found in stem cell niches. Furthermore, TCs were found accompanying cardiomyocyte progenitor cells in different stages of development [40]. Our results demonstrated that TCs are located close to tubules and blood capillaries in the kidney cortex. The presence of extracellular vesicles is considered an important pathway of cell interaction [42–44]. Extracellular vesicles, in very close vicinity to the cellular bodies of TCs or at different levels of Tps, have been described by Popescu *et al.* in other organs [3, 8, 10, 11, 14, 16, 19]. This suggests the interactions of TCs with neighbouring cells. Our TEM images also show extracellular vesicles of TCs within the kidney interstitium, suggesting that kidney TCs are also involved in cell-to-cell communication, protection, information exchange and so on [45], through a paracrine/juxtacrine mechanism.

Acknowledgements

Conflict of interest

The authors declare no conflict of interest.

References

1. **Popescu LM, Faussone-Pellegrini MS.** TELOCYTES - a case of serendipity: the winding way from Interstitial Cells of Cajal (ICC), via Interstitial Cajal-Like Cells (ICLC) to TELOCYTES. *J Cell Mol Med*. 2010; 14: 729–40.

2. **Kostin S.** Myocardial telocytes: a specific new cellular entity. *J Cell Mol Med*. 2010; 14: 1917–21.

3. **Popescu LM, Manole CG, Gherghiceanu M, et al.** Telocytes in human epicardium. *J Cell Mol Med*. 2010; 14: 2085–93.

4. **Gherghiceanu M, Manole CG, Popescu LM.** Telocytes in endocardium: electron microscope evidence. *J Cell Mol Med*. 2010; 14: 2330–4.

5. **Suciu L, Nicolescu MI, Popescu LM.** Cardiac telocytes: serial dynamic images in cell culture. *J Cell Mol Med*. 2010; 14: 2687–92.

6. **Suciu L, Popescu LM, Gherghiceanu M, et al.** Telocytes in human term placenta: morphology and phenotype. *Cells Tissues Organs*. 2010; 192: 325–39.

7. **Cantarero Carmona I, Luesma Bartolome MJ, Junquera Escribano C.** Identification of telocytes in the lamina propria of rat duode-num: transmission electron microscopy. *J Cell Mol Med*. 2011; 15: 26–30.

8. **Popescu LM, Manole E, Serboiu CS, et al.** Identification of telocytes in skeletal muscle interstitium: implication for muscle regeneration. *J Cell Mol Med*. 2011; 15: 1379–92.

9. **Zheng Y, Li H, Manole CG, et al.** Telocytes in trachea and lungs. *J Cell Mol Med*. 2011; 15: 2262–8.

10. **Cantarero I, Luesma MJ, Junquera C.** The primary cilium of telocytes in the vasculature: electron microscope imaging. *J Cell Mol Med*. 2011; 15: 2594–600.

11. **Hinescu ME, Gherghiceanu M, Suciu L, et al.** Telocytes in pleura: two- and three-dimensional imaging by transmission electron microscopy. *Cell Tissue Res*. 2011; 343: 389–97.

12. **Rusu MC, Pop F, Hostiuc S, et al.** The human trigeminal ganglion: c-kit positive neurons and interstitial cells. *Ann Anat*. 2011; 193: 403–11.

13. **Cretoiu SM, Simionescu AA, Caravia L, et al.** Complex effects of imatinib on spontaneous and oxytocin-induced contractions in human non-pregnant myometrium. *Acta Physiol Hung*. 2011; 98: 329–38.

14. **Hatta K, Huang ML, Weisel RD, et al.** Culture of rat endometrial telocytes. *J Cell Mol Med*. 2012; 16: 1392–6.

15. **Ceafalan L, Gherghiceanu M, Popescu LM, et al.** Telocytes in human skin - are they involved in skin regeneration? *J Cell Mol Med*. 2012; 16: 1405–20.

16. **Gevaert T, De Vos R, Van Der Aa F, et al.** Identification of telocytes in the upper lamina propria of the human urinary tract. *J Cell Mol Med*. 2012; 16: 2085–93.

17. **Nicolescu MI, Bucur A, Dinca O, et al.** Telocytes in parotid glands. *Anat Rec (Hoboken)*. 2012; 295: 378–85.

18. **Popescu BO, Gherghiceanu M, Kostin S, et al.** Telocytes in meninges and choroid plexus. *Neurosci Lett*. 2012; 516: 265–9.

19. **Nicolescu MI, Popescu LM.** Telocytes in the interstitium of human exocrine pancreas: ul-

trastructural evidence. *Pancreas*. 2012; 41: 949–56.

20. **Cretoiu D, Cretoiu SM, Simionescu AA, et al.** Telocytes, a distinct type of cell among the stromal cells present in the lamina propria of jejunum. *Histol Histopathol*. 2012; 27: 1067–78.

21. **Tanaka T, Nangaku M.** Pathogenesis of tubular interstitial nephritis. *Contrib Nephrol*. 2011; 169: 297–310.

22. **Vitalone MJ, Naesens M, Sigdel T, et al.** The dual role of epithelial-to-mesenchymal transition in chronic allograft injury in pediatric renal transplantation. *Transplantation*. 2011; 92: 787–95.

23. **Lee S, Huen S, Nishio H, et al.** Distinct macrophage phenotypes contribute to kidney injury and repair. *J Am Soc Nephrol*. 2011; 22: 317–26.

24. **Kaissling B, Le Hir M.** The renal cortical interstitium: morphological and functional aspects. *Histochem Cell Biol*. 2008; 130: 247 –62.

25. **Boor P, Floege J.** The renal (myo-)fibroblast: a heterogeneous group of cells. *Nephrol Dial Transplant*. 2012; 27: 3027– 36.

26. **Berg EL, Mullowney AT, Andrew DP, et al.** Complexity and differential expression of carbohydrate epitopes associated with L-selectin recognition of high endothelial venules. *Am J Pathol*. 1998; 152: 469–77.

27. **Nielsen JS, McNagny KM.** Novel functions of the CD34 family. *J Cell Sci*. 2008; 121: 3683–92.

28. **Lebduska P, Korb J, Tumova M, et al.** Topography of signaling molecules as detected by electron microscopy on plasma membrane sheets isolated from non-adherent mast cells. *J Immunol Methods*. 2007; 328: 139–51.

29. **Cismasiu VB, Radu E, Popescu LM.** miR-193 expression differentiates telocytes from other stromal cells. *J Cell Mol Med*. 2011; 15: 1071–4.

30. **Manole CG, Cismasiu V, Gherghiceanu M, et al.** Experimental acute myocardial infarction: telocytes involvement in neo-angiogenesis. *J Cell Mol Med*. 2011; 15: 2284–96.

31. **Zheng Y, Bai C, Wang X.** Telocyte morphologies and potential roles in diseases. *J Cell Physiol*. 2012; 227: 2311–7.

32. **Zheng Y, Bai C, Wang X.** Potential significance of telocytes in the pathogenesis of lung diseases. *Expert Rev Respir Med*. 2012; 6: 45–9.

33. **Faussone-Pellegrini MS, Bani D.** Relationships between telocytes and cardiomyocytes during pre- and post-natal life. *J Cell Mol Med*. 2010; 14: 1061–3.

34. **Bani D, Formigli L, Gherghiceanu M, et al.** Telocytes as supporting cells for myocardial tissue organization in developing and adult heart. *J Cell Mol Med*. 2010; 14: 2531–8.

35. **Zhou J, Zhang Y, Wen X, et al.** Telocytes accompanying cardiomyocyte in primary culture: two- and three-dimensional culture environment. *J Cell Mol Med*. 2010; 14: 2641–5.

36. **Gherghiceanu M, Popescu LM.** Heterocellular communication in the heart: electron tomography of telocyte-myocyte junctions. *J Cell Mol Med*. 2011; 15: 1005–11.

37. **Popescu LM, Gherghiceanu M, Suciu LC, et al.** Telocytes and putative stem cells in the lungs: electron microscopy, electron tomography and laser scanning microscopy. *Cell Tissue Res*. 2011; 345: 391–403.

38. **Gherghiceanu M, Popescu LM.** Cardiac telocytes - their junctions and functional implications. *Cell Tissue Res*. 2012; 348: 265–79.

39. **Rusu MC, Pop F, Hostiuc S, et al.** Telocytes form networks in normal cardiac tissues. *Histol Histopathol*. 2012; 27: 807–16.

40. **Gherghiceanu M, Popescu LM.** Cardiomyocyte precursors and telocytes in epicardial stem cell niche: electron microscope images. *J Cell Mol Med*. 2010; 14: 871–7.

41. **Bojin FM, Gavriliuc OI, Cristea MI, et al.** Telocytes within human skeletal muscle stem cell niche. *J Cell Mol Med*. 2011; 15: 2269–72.

42. **Murphy AS, Peer WA.** Vesicle Trafficking: ROP-RIC Roundabout. *Curr Biol*. 2012; 22: R576–8.

43. **Guduric-Fuchs J, O'Connor A, Camp B, et al.** Selective extracellular vesicle-mediated export of an overlapping set of microRNAs from multiple cell types. *BMC Genomics*. 2012; 13: 357.

44. **Brenner MP.** Endocytic traffic: vesicle fusion cascade in the early endosomes. *Curr Biol*. 2012; 22: R597–8.

45. **Nieuwland R, Sturk A.** Why do cells release vesicles? *Thromb Res*. 2010; 125(Suppl. 1): S49–51.